Published in final edited form as:

*IEEE Trans Med Imaging*. 2007 April ; 26(4): 582–597. doi:10.1109/TMI.2007.892499.

# Cortical Surface Shape Analysis Based on Spherical Wavelet Transformation

**Peng Yu**[1], **Xiao Han**[2], **Florent Ségonne**[3,4], **Rudolph Pienaar**[3], **Randy L. Buckner**[3,5,6], **Polina Golland**[4], **P. Ellen Grant**[3,7], and **Bruce Fischl**[1,3,4]

[1]Health Science and Technology, MIT, Cambridge, MA, 02139

[2]CMS Inc., St. Louis, MO, 63132

[3]Athinoula A. Martinos Center for Biomedical Imaging, MGH/MIT/HMS, Charlestown, MA, 02129

[4]CSAIL, MIT, Cambridge, MA, 02139

[5]Department of Psychology, Harvard University, Cambridge, MA, 02138

[6]Department of Radiology, Harvard Medical School, Boston, MA, 02115

[7]Pediatric Radiology, Massachusetts General Hospital, Boston, MA, 02114

## Abstract

Shape analysis of neuroanatomical structures has proven useful in the study of neuropathology and neurodevelopment. Advances in medical imaging have made it possible to study this shape variation in vivo. In this paper, we propose the use of a spherical wavelet transformation to extract cortical surface shape features, as wavelets can characterize the underlying functions in a local fashion in both space and frequency. Our results demonstrate the utility of the wavelet approach in both detecting the spatial scale and pattern of shape variation in synthetic data, and for quantifying and visualizing shape variations of cortical surface models in subject populations.

## 1. Introduction

Evidence suggests that morphological changes of neuroanatomical structures may reflect abnormalities in neurodevelopment, or a variety of disorders, such as schizophrenia and Alzheimer's Disease (AD). These morphological variations can be characterized by the change of volume and shape. Efforts have originally been made to verify the relationship between the pathology and the volumetric variation of various neuroanatomical subjects, such as the cerebral cortex, hippocampus and corpus callosum. Recently, a considerable amount of effort has been focused on developing a technique to quantify the changes in the 2D or 3D shape of brain structures, which could potentially lead to more accurate diagnoses, better treatments, and an improved understanding of neurodevelopment.

To accurately study inter-subject shape variations, one would like to find not only an effective shape representation but also a registration method to preserve individual variation

while aligning anatomically important structures. Different techniques employed in these two aspects confer merits and disadvantages to various shape analysis methods. One of the earliest techniques developed in this field represented shape by points sampled on the boundary of the object being studied, and the coordinates of the corresponding points on different subjects were directly used as shape features [1, 2]. Cootes et al. extended this method by building the point distribution model, which allows for global scale analysis of shape variation by applying principal component analysis (PCA) to the positions of the boundary points [3]. However, this method depends heavily on the accuracy of the inter-subject registration for group comparison. Subsequently, parametric models were developed to decompose the boundary or surface using Fourier descriptor and spherical harmonics descriptor, and to use the decomposition coefficients as shape descriptor [4–7]. A drawback of these models is the lack of ability to study local shape variation because of the global support of the basis functions. Another popular method warps a template to individual subjects and studies the deformation field for shape variations [8–11]. Although this method is sensitive to the template selection and presents challenges in interpreting and comparing shape differences using the high-dimensional deformation field, a number of interesting shape analysis results have been obtained and more advanced techniques based on it have been developed. Medial axis technique, originally proposed by Pizer et al. and Golland et al. in 3D and 2D, respectively, has been applied as a powerful tool for the shape analysis of a variety of subcortical structures [12, 13]. This technique allows for the separate study of the local position and thickness of the object at both coarse and fine levels. Another advantage of medial descriptions is due to the object intrinsic coordinate system, which facilitates the construction of correspondences between surfaces and further statistical study. However, a fundamental problem of any skeletonization technique is sensitivity to perturbations in the boundary, which presents a challenge to the further development and application of medial representation.

In order to accurately and efficiently extract shape features and conduct statistical analysis, we developed a procedure to decompose a surface using spherical wavelets, which can characterize the underlying functions in a local fashion in both space and frequency. Principal component analysis was further applied to the wavelet coefficients to build shape models and study the main modes of shape variation within a group of subjects in separate spatial-frequency domains. The entire procedure and various steps involved in this study are introduced in detail in the Methods section. The results of using this procedure in detecting the spatial scale and pattern of shape variation in a set of synthetic data are demonstrated in the Results section. The use of PCA in studying multi-resolutional cortical shape variations in healthy aged population and neonates is also presented.

## 2. Methods

In this section, the tools used for preprocessing the cortical surfaces are introduced, and the procedures developed for conducting wavelet transformation and further statistical analysis using PCA are also presented.

### 2.1. Preprocessing

For decomposing a surface using basis functions defined in the spherical coordinate system, such as spherical wavelets, the surface has to be mapped onto a parameterized sphere. In order to carry out any statistical analysis on the corresponding points across subjects, surfaces need to be registered properly. A set of largely automated tools developed by FreeSurfer group are used to pre-process the data, which includes cortical surface reconstruction, spherical transformation and inter-subject registration in the spherical coordinates based on the folding pattern of cortical surfaces [14, 15].

To reconstruct the cortical surfaces, which include the gray/white matter boundaries and gray-matter/CSF boundaries of the left and right hemispheres, the MR images are first registered to a pre-built template in the Talairach space. The image intensity is then normalized and used to guide skull stripping and white matter labeling. This white matter segmentation is further refined and cut to generate a single connected mass of each hemisphere. The surface of the labeled white matter of each hemisphere is then tessellated by using eight triangles to represent each square face of the voxel in the interface between white matter and differently labeled voxels. For generating a more accurate and smoother white matter surface, this tessellation is refined and deformed in the normalized image volume under smoothness and pre-calculated boundary intensity constraints. Furthermore, the white matter surface is deformed outwards to the location in the volume that has the biggest intensity contrast between the gray matter and CSF, and refined to generate the pial surface. Finally, topological defects are automatically detected and corrected for both surfaces to guarantee the topology of a sphere.

Each reconstructed cortical surface of each subject is first mapped onto a sphere with minimal metric distortion, and then registered in the spherical coordinate system with a balance of the exactness of the folding pattern's alignment and the introduced distortion, using a combination of a topology preserving term, a folding alignment term and a metric preserving term. This alignment enables us to find anatomically corresponding points on the reconstructed cortical surfaces across subjects.

### 2.2. Spherical wavelets

Broadly speaking, a wavelet representation of a function consists of a coarse overall approximation together with more detailed coefficients that influence the function at various resolutions and locations. The classical form of wavelet analysis decomposes signals using a set of basis functions, called wavelets, in which every wavelet is just a scaled and translated copy of a single unique function, called the mother wavelet. However, this shift-invariant theory breaks down when representing data sets on a bounded surface. The newly developed biorthogonal spherical wavelet basis functions are based on recursive subdivision starting with an icosahedron and a lifting scheme. The fast wavelet transformation algorithm developed allows for the efficient and accurate decomposition of any function on the sphere [16]. The coordinates vector $v = (x, y, z)^T$, where x, y, z are coordinates on the original surface, for example, is such a function and can be expanded by a set of spherical wavelet functions as

$$\overline{v}=\sum_{j,k}\overline{\gamma}_{j,k}\psi_{j,k} \quad (1)$$

where $\overline{\gamma}_{j,k}$ are the 3-dimensional coefficients at level $j$, $j = -1,0,\ldots l$ and location $k$, $k \in M(j)$. These coefficients can be used as shape features because each provides some limited information about both the position and the frequency of the decomposed surface (Figure 1).

However, in order to make these shape features invariant to rotation, translation and scaling, the coordinate functions have to be normalized with respect to a reference coordinate frame. This normalization is initialized first by transforming each surface using the transformation matrix calculated previously for volume Talairach registration during surface reconstruction. The roughly normalized coordinates of corresponding points on all the surfaces, where the correspondence is found by the spherical registration, are averaged to create a new template surface for the second round normalization. Then, each surface is normalized by finding an optimal linear transformation that minimizes the mean square error of the transformed individual surface and the template.

These normalized wavelet coefficients provide a way to study shape variations hierarchically. To test this ability, five synthetic cortical surfaces were generated by making a bump on a template surface at the same location, but with increasing height. PCA was applied to the separate frequency levels to detect pattern of shape variations caused by this synthetic deformation, as described in the following sections.

### 2.3. Principal Component Analysis

Principal Component Analysis is a useful tool in finding patterns in data of high dimension. It has been extensively used in the fields of computer vision and image recognition. Based on this technique, methods have been developed to build generative models of shape variation within a single population and used to segment 2D or 3D medical images [17–19]. The basic idea of these approaches is to identify and visualize the first few principal modes of the variation of the positions of points on the boundary or surface of the dataset.

For example, if $x_i (i = 1, \cdots N)$ is a vector containing shape features, such as the coordinates of the points on the surface calculated for a group of subjects, then any individual shape can be decomposed as:

$$x_i=\overline{x}+\sum_{j=1}^{N}e_j e_j^T(x_i-\overline{x}), \quad (2)$$

where $\overline{x}$ is the mean of $x_i (i = 1, \cdots N)$, $e_1, \cdots, e_N$ are the eigenvectors corresponding to eigenvalues $\lambda_1, \lambda_2, \cdots, \lambda_N$ of the covariance matrix of $x$, in decreasing order. This is essentially equivalent to linearly transforming a dataset into a new coordinate system such that the variance of the projection of the dataset on the first axis (first principal component) is greatest, and the variance of projection on the second axis is the second greatest, and so on. The fact that the variance explained by each eigenvector is equal to the corresponding eigenvalue enables us to study the most significant modes of variation in the dataset. Usually, most of the variations can sufficiently be represented by a small number of modes,

k, so that the sum of the first k variances represents a sufficiently large proportion of total variance of all the variables used to derive the covariance matrix. Thus by limiting the number of terms in equation 2, the statistical analysis can be greatly simplified. However, it has been argued that omitting the eigenvectors corresponding to relatively small shape variations leads to the failure of characterizing subtle, yet important shape features because coordinates of all the points on the surface are collected in the shape feature vector [20]. For the same reason, the application of PCA in the shape study of neuroanatomical structures (i.e. the cortical surface) has also been largely limited.

In this work, we propose to conduct PCA on wavelet coefficients at different frequency levels separately, as the coefficients in the lowest level provide an overall approximation and localized morphological variations are captured hierarchically by the higher-level coefficients. Instead of using positions of all the points on the surface as shape feature in equation 2, each time we take only $x_{il} = (c_{i,N(l-1)+1}, \cdots c_{i,N(l)})^T$, the subset of the wavelet coefficients in one frequency level as input, where $N(l)$ is the number of coefficients up to level $l = 0,\ldots 7$. Once the set of principal components $e_{lj} (j = 1, \cdots k \leq N)$ that characterizes the majority of the variance of the wavelet coefficients in the $l^{th}$ frequency level is found, the corresponding shape variations can be visualized by inversely transforming the principal components to generate the principal surfaces. This visualization technique provides an intuitive way to analyze and understand the most distinct patterns of shape variations within a group of subjects from coarse to fine resolution.

### 2.4. Data

Two sets of high-resolution structural MR scans were analyzed in this paper. The first dataset was obtained from a total of 84 nondemented older participants (OP; 42 women: 67–95, mean age = 80, standard derivation = 7.25; 42 men: 71–94, mean age = 79, standard derivation = 7.17). These data have been reported previously in several publications associated with the Washington University Alzheimer's Disease Research Center (ADRC). None of the participants had any history of neurologic, psychiatric, or medical illness that could contribute to dementia or a serious medical condition. Two to four high-resolution MP-RAGE scans were motion corrected and averaged per participant (four volumes were averaged for all except five participants; Siemens 1.5T Vision System, resolution 1 × 1 × 1.25 mm, TR = 9.7 ms, TE = 4 ms, FA = 10°, TI = 20 ms, TD = 200 ms) to create a single high contrast-to-noise image volume. These acquisition parameters were empirically optimized to increase gray/white and gray/cerebrospinal fluid contrast. Cortical surfaces were reconstructed and registered as described in previous section. This dataset was mainly used to study normal variations and aging-related shape changes of gray/white matter boundaries in a healthy older population. Five female participants, all around 71, were selected, and the average of their cortical surfaces was used as the template for generating synthetic data.

The second dataset was from five normal neonates with corrected gestational ages (cGA) of 31.1, 34, 38.1, 38.4, and 39.72 weeks. T1 weighted 3D SPGR images were collected on a 1.5T scanner, with TR/TE = 30/8, flip angle = 25 to 30 degrees, matrix = 256×192, FOV = 220×165 mm or 200 × 150 mm and slice thickness 1.2 to 1.4 mm. Resultant DICOMS were

manually segmented into white matter and cortical regions. Wavelet transformation and PCA are then applied to the reconstructed gray/white matter boundary to study the shape changes of cortical surface in neurodevelopment.

## 3. Results

### 3.1. Shape Pattern Recognition in Synthetic Data

The top row in Figure 2 shows the five synthetic cortical surfaces, each with a bump located in the same region around the anterior tip of the temporal lobe. The deformation was made by moving each vertex in the deformation region outward along its normal direction by a certain distance, which increases from 0 mm for the first surface to 2 mm for the last surface. These five synthetic surfaces were registered and transformed into the wavelet domain as described in the Methods section. The PCA study of the wavelets coefficients shows that about 98% of the shape variations were accounted for by the first principle component at all the frequency levels. To visualize the shape changes captured by the first principle component at each level, we first construct a subset of projected wavelet coefficients for each surface as:

$$x_{il}^{projected} = \bar{x}_l + e_{l1} e_{l1}^T (x_{il} - \bar{x}_l) \quad (3)$$

where $x_{il}$ is the subset of wavelet coefficients of the $i^{th}$ surface at $l^{th}$ level, $\bar{x}_l$ is the averaged wavelet coefficients of all the surfaces at $l^{th}$ level, and $e_{l1}$ is the first eigenvector calculated at $l^{th}$ level. Then the whole set of projected wavelet coefficients is constructed by filling in the other levels with the first surface's wavelet coefficients. Figure 2 illustrates the surfaces that result from taking inverse wavelet transformation of these projected wavelet coefficients from low to high levels, with color indicating the magnitude and spatial coverage of each wavelet coefficient in $e_{l1} e_{l1}^T (x_{il} - x_{1l})$. It is shown that the overall shape change of the temporal lobe caused by the synthetic deformation is captured exclusively at the low frequency level (2nd row in Figure 2). The smaller scale shape change of the secondary folds on the temporal lobe is characterized by the middle frequency level (3rd row in Figure 2). And the shape variation on the sharp edge of the bump is identified at the high frequency level (bottom row in Figure 2).

### 3.2. Shape Variation in Aged Normal Population

The PCA study of the wavelet coefficients in the nondemented older sample demonstrated a wide range of differences of cortical surface geometry, in both the overall shape of the cortex and the hierarchically finer local details. Most of the shape variance (98%) is represented by the first 10 to 20 eigenvectors and the variance explained by the first principal component ranges from 8% to 13% of the total variance at the lower spatial-frequency levels. Variances in higher frequency scales spread out more evenly over 50 to 80 eigenvectors. The shape variation represented by the $j^{th}$ principal component at $l^{th}$ frequency level is illustrated by generating two sets of new wavelet coefficients:

$$x_{lj\pm} = \bar{x}_l \pm 3\sigma_{lj} e_{lj}, \quad (4)$$

where $\bar{x}_l$ is the mean wavelet coefficients of all the subjects at $l^{th}$ level, $\sigma_{l,j}^2$ is the $j^{th}$ eigenvalue of the covariance matrix of the wavelet coefficients at level $l$. Mean wavelet coefficients were used in the other levels to generate the whole set of wavelet coefficients. By inversely transforming these two sets of wavelet coefficients, two synthetic surfaces can be generated, and the difference between them represents the shape variations characterized by the corresponding eigenvector at different frequency levels. Figure 3 shows the generated surfaces for level 0 to 5 with color indicating the magnitude, location and spatial scale of each coefficient in vector $e_{lj}$.

Moreover, a preliminary study of cortical shape (gray/white matter boundary) variations due to healthy aging was carried out by observing the change with age of the projected surfaces on the set of eigenvectors representing 98% of the variances at each level. The projected surface of the $i^{th}$ subject at $l^{th}$ level is reconstructed by inversely transforming the projected wavelet coefficients calculated using equation 3, but with other levels filled with the mean wavelet coefficients.

Shape changes consistent with age were observed in the low-frequency domain as well. Figure 4 shows the projected cortical surfaces in three age ranges of female and male subjects using second level wavelet coefficients. The narrowing of the central sulcus and the elongation of the occipital lobe with aging were both observed in female and male groups, which may characterize and correlate with white matter atrophy. More rigorous study needs to be carried out to verify this result.

### 3.3. Shape Variation in Neonates

Using the wavelet decomposition technique, the major cortical surface variations related to neurodevelopment in a small population of nenoates are identified to be in the middle spatial-frequency domain. PCA is used to study the specific modes of shape variations correlated with corrected gestational age. PCA of the wavelet coefficients shows that more than 98% of the shape variations are represented by the first three principal components at every frequency level. Projected surfaces are reconstructed to study the shape variations represented by each of the first three principal components at each frequency level separately, using equation 3. The set of coefficients of the youngest subject (31.1 weeks gestational age) is used to fill in the other levels to build the whole set of projected coefficients at each level. As shown in Figure 5, the reconstructed surfaces (using wavelet coefficients projected on the first principal component) with age demonstrate the increasing folding of the gray/white matter boundary of the left hemisphere at level 4. Shape variations presented at the lower spatial resolution, which are not correlated with age, are believed to reflect normal brain variation.

## 4 Discussion and future work

Spherical wavelet transformations are demonstrated to accurately and efficiently detect the locations and spatial scales of shape variations. The use of principal component analysis on wavelet coefficients provides a novel way to detect and visualize modes of shape variation in a set of subjects. Application of this method in the cortical shape study shows promising results regarding the specific patterns and spatial scales of variations correlated with

nondemented aging and neurodevelopment. Future work includes employing advanced statistical tools and extending the wavelet analysis to other neuroanatomical structures.

## Acknowledgments

Support for this research was provided in part by the NCRC (P41-RR14075, R01 RR16594-01A1 and the NCRR Morphometric Project BIRN002, U24 RR021382), the NIBIB (R01 EB001550), NIA Grants P50 AG05681 and P01 AG03991, NAMIC NIH NIBIB U54-EB005149, NIH NINDS R01-NS051826 and K23 NS42758. The authors also would like to thank Washington University ADRC and the MIND Institute.

## References

1. Dryden I, Mardia K. Multivariate shape analysis. Sankhya. 1993; 55:460–480.
2. Bookstein FL. Morphometric Tools for Landmark Data: Geometry and Biology. 1991
3. Cootes T, Taylor C, Cooper D, Graham J. Active shape models - their training and application. Computer Vision and Image Understanding. 1995; 61:38–59.
4. Brechbüler C, Gerig G, Kübler O. Parametrization of Closed Surfaces for 3-D Shape Description. Computer Vision and Image Understanding. 1995; 61:154–170.
5. Kelemen A, Székely G, Gerig G. Elastic model-based segmentation of 3d neuroradiological data sets. IEEE Transactions on Medical Imaging. 1999; 18:828–839. [PubMed: 10628943]
6. Styner M, Gerig G, Lieberman J, Jones D, Weinberger D. Statistical shape analysis of neuroanatomical structures based on medial models. Medical Image Analysis. 2003; 7:207–220. [PubMed: 12946464]
7. Shen L, Ford J, Makedon F, Saykin A. hippocampal shape analysis surface-based representation and classification. SPIE Medical Imaging. 2003
8. Christensen G, Rabbitt R, Miller M. 3d brain mapping using a deformable neuroanatomy. Physics in Medicine and Biology. 1994; 39:609–618. [PubMed: 15551602]
9. Davatzikos C, Vaillant M, Resnick S, Prince J, Letovsky S, Bryan R. A computerized method for morphological analysis of the corpus callosum. Journal of Computer Assisted Tomography. 1996; 20:88–97. [PubMed: 8576488]
10. Joshi SC, Miller MI, Grenander U. On the geometry and shape of brain sub-manifolds. IJPRAI. 1997; 11:1317–1343.
11. Thompson P, Giedd J, Woods R, MacDonald D, Evans A, Toga A. Growth patterns in the developing brain detected by using continuum machanical tensor maps. Nature. 2000:190–193. [PubMed: 10724172]
12. Pizer S, Fritsch D, Yushkevich P, Johnson V, Chaney E. Segmentation, registration, and measurement of shape variation via image object shape. IEEE Transactions on Medical Imaging. 1999; 18:851–865. [PubMed: 10628945]
13. Golland P, Grimson W, Kikinis R. Statistical shape analysis using fixed topology skeletons: Corpus callosum study. Information Processing in Medical Imaging. 1999:382–388.
14. Dale AM, Fischl B, Sereno MI. Cortical surface-based analysis. I. Segmentation and surface reconstruction. Neuroimage. 1999; 9:179–94. [PubMed: 9931268]
15. Fischl B, Sereno MI, Dale AM. Cortical surface-based analysis. II: Inflation, flattening, and a surface-based coordinate system. Neuroimage. 1999; 9:195–207. [PubMed: 9931269]
16. Schröder P, Sweldens W. Spherical wavelets: Efficiently representing functions on a sphere. Computer Graphics Proceedings (SIGGRAPH 95). 1995:161–172.
17. Cootes, TF.; Taylor, CJ.; Cooper, DH.; Graham, J. Proc British Machine Vision Conference. Springer-Verlag; 1992. Training Models of Shape from Sets of Examples; p. 9-18.
18. Székely G, et al. Segmentation of 2D and 3D objects from MRI volume data using constrained elastic deformations of flexible Fourier contour and surface models. Medical Image Analysis. 1996; 1:19–34. [PubMed: 9873919]
19. Leventon ME, Grimson WEL, Faugeras O. Statistical Shape Influence in Geodesic Active Contours. Proc CVPR'2000. 2000:316–323.

20. Shen D, Davatzikos C. An Adaptive-Focus Deformable Model Using Statistical and Geometric Information. IEEE Transactions on Pattern Analysis and Machine Intelligence. 2000; 22:906–913.

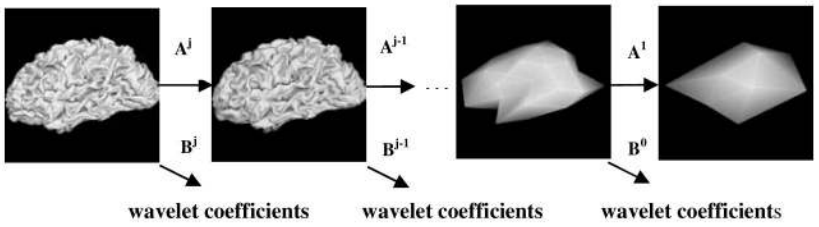


**Figure 1.**
Wavelet decomposition of cortical surface

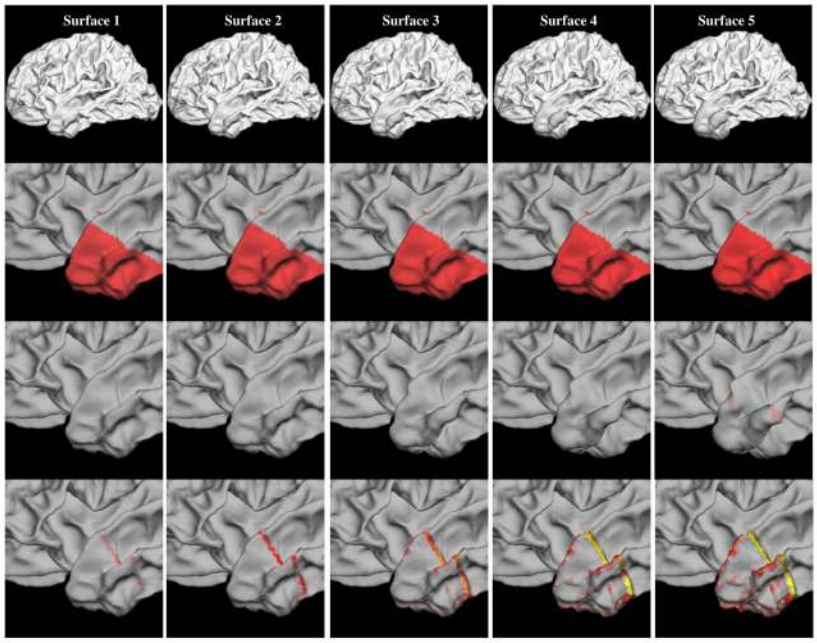


**Figure 2.**

Shape pattern recognition in synthetic data: The synthetic surfaces are in first row; The reconstructed surfaces using projected wavelet coefficients at level 1, 4 and 6 are in 2nd, 3rd and bottom rows respectively (Colormap indicating the magnitude and spatial scale of shape variation detected by PCA).

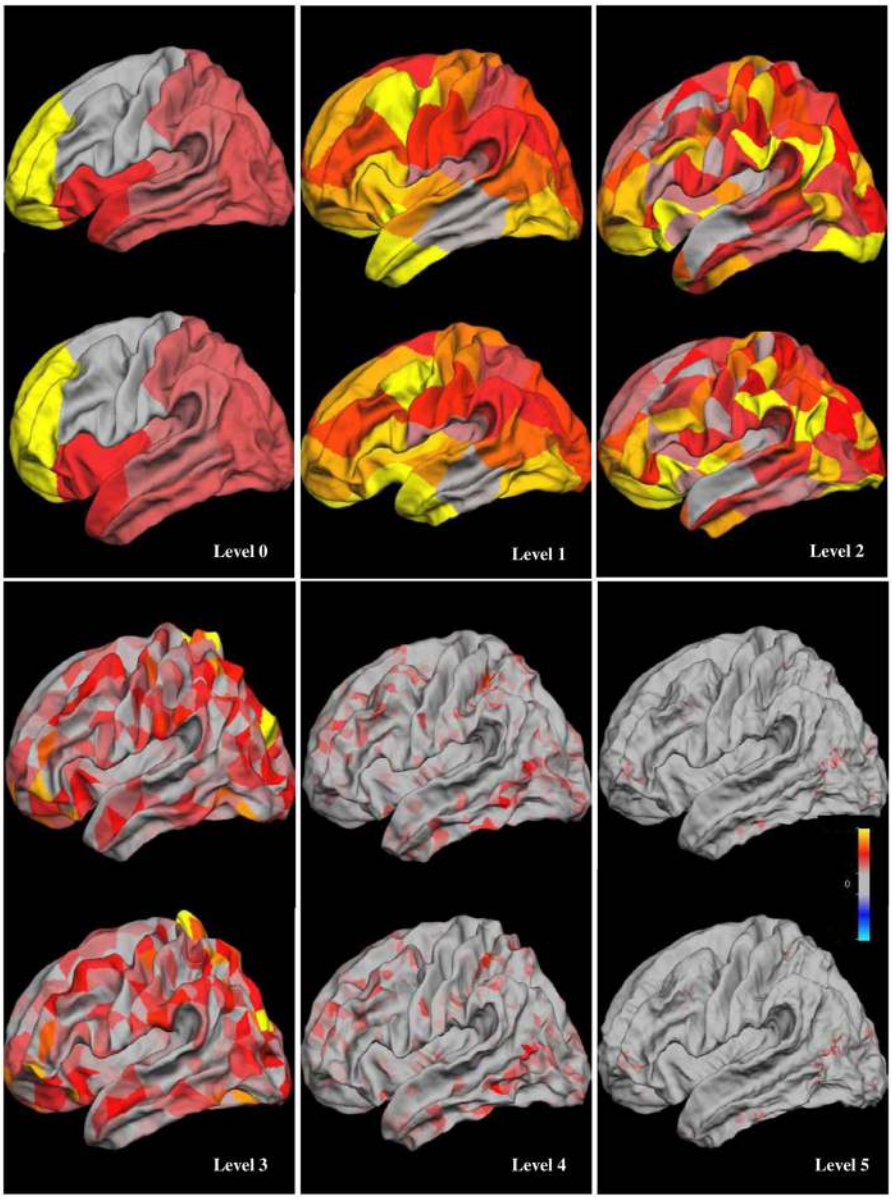


**Figure 3.**

The principal surfaces representing the $\mp 3\sigma$ variations (ordered in top-down direction) of the first principal component at level 0 to 5: color showing the spatial scale and magnitude of each wavelet coefficients in the first principle component.

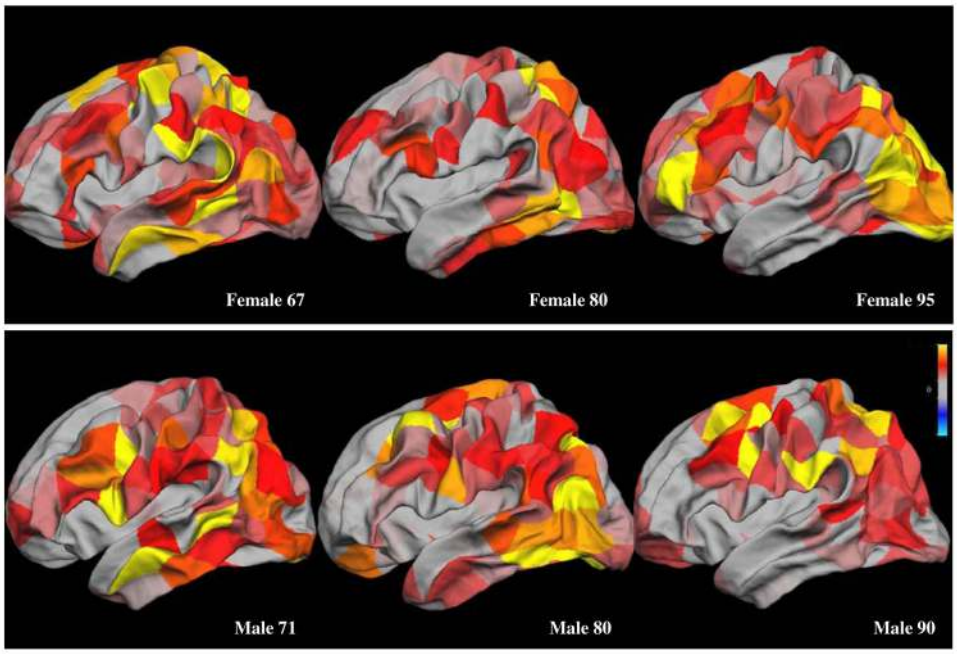


**Figure 4.**

Reconstructed surfaces for female and male subjects of different ages using projected wavelet coefficients on the set of principal components that represent 98% of the total variance at level 2.

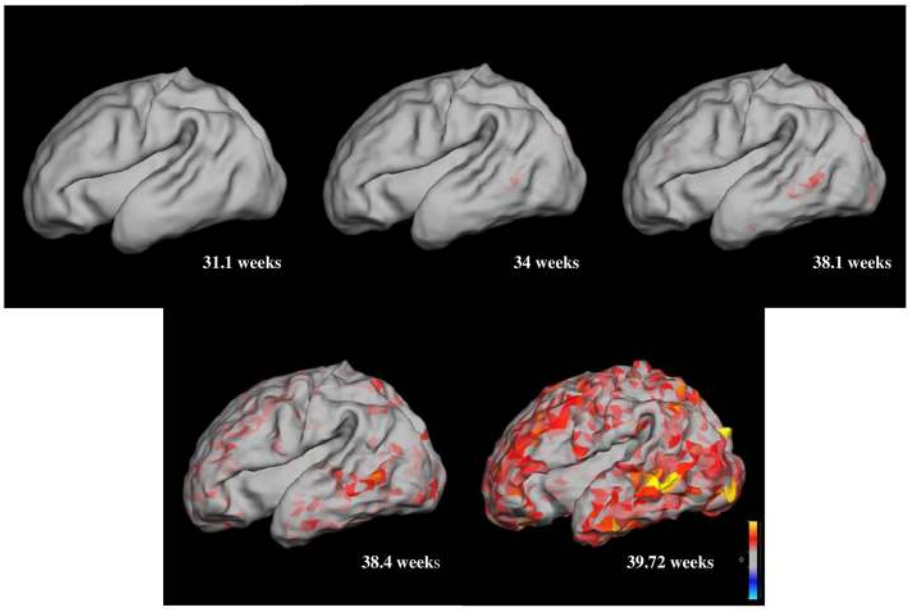


**Fig. 5.**

Reconstructed gray/white matter surfaces of neonates ordered with cGA using projected wavelet coefficients on the first principal component of wavelet coefficients at level 4.